

A comparison of information value and logistic regression models in landslide susceptibility mapping by using GIS

Tao Chen¹ · Ruiqing Niu¹ · Xiuping Jia²

Received: 24 June 2015 / Accepted: 24 November 2015 / Published online: 10 May 2016
© Springer-Verlag Berlin Heidelberg 2016

Abstract This study investigates the application of information value (InV) and logistic regression (LR) models for producing landslide susceptibility maps (LSMs) of the Zigui–Badong area near the Three Gorges Reservoir in China. This area is subject to anthropogenic influences because the reservoir’s water level cyclically fluctuates between 145 and 175 m. In addition, the area suffers from extreme rainfall events due to the local climate and has experienced significant and widespread landslide events in recent years. In this study, a landslide inventory map was initially constructed using field surveys, aerial photographs, and a literature search of historical landslide records. Eight causative factors, including lithology, bedding structure, slope, aspect, elevation, profile curvature, plane curvature, and fractional vegetation cover, were then considered in the generation of LSMs by using the InV and LR models. Finally, the prediction performances of these maps were assessed through receiver operating characteristics (ROC) that utilized both success-rate and prediction-rate curves. The validation results showed that the area under the ROC curve for the InV model was 0.859 for the success-rate curve and 0.865 for prediction-rate curve; these results

indicate the InV model surpassed the LR model (0.742 for success-rate curve and 0.740 for prediction-rate curve). Overall, the two models provided nearly similar results. The results of this study show that landslide susceptibility mapping in the Zigui–Badong area is viable with both approaches.

Keywords Landslide susceptibility models · The Three Gorges Reservoir · GIS · Logistic regression · Information value model

Introduction

More than 3800 landslide locations have been reported in the area near the Three Gorges Reservoir along the Yangtze River in China (Liu et al. 2009), which poses a serious threat to the socioeconomic stability of the region. The instability of bank slopes is a serious and inevitable problem due to the significant increases and periodic fluctuations in the water level of the reservoir. Therefore, landslide prediction is critical for landslide prevention and mitigation in this area.

Landslide susceptibility mapping (LSM) is a complex task (Brabb 1991). Numerous approaches for producing landslide susceptibility maps (LSMs) have been developed that can be grouped into three broad categories: statistical, soft computing, and analytic methods (Pradhan 2013). The application of analytic methods is most difficult when the study area is large. For this reason, the use of statistical and soft computing methods has steadily increased. Moreover, the implementation of these methods in geographical information systems (GIS) is a relatively easy task.

Over the last decade, several studies have examined indirect LSM by using a statistical approach (Guzzetti et al.

This article is part of a Topical Collection in Environmental Earth Sciences on “Environmental Research of the Three Gorges Reservoir,” guest edited by Binghui Zheng, Shengrui Wang, Yanwen Qin, Stefan Norra, and Xiafu Liu.

✉ Ruiqing Niu
417519023@qq.com

¹ Institute of Geophysics and Geomatics, China University of Geosciences, Wuhan, People’s Republic of China

² School of Engineering and Information Technology, University of New South Wales, Canberra, ACT 2610, Australia

1999; Lee and Pradhan 2007; Nefeslioglu et al. 2008; Bai et al. 2008, 2009, 2010; Akgun and Turk 2010; Pradhan 2010; Pradhan et al. 2011; Akgun et al. 2011; Bathrellos et al. 2012, 2013; Papadopoulou-Vrynioti et al. 2013; Youssef and Maerz 2013; Chen et al. 2015). Various methods have been proposed, including the information value (InV) (Ramakrishnan et al. 2005; Vijith et al. 2009; Balasubramani and Kumaraswamy 2013; Sarkar et al. 2013) and the logistic regression (LR) methods (Yesilnacar and Topal 2005; Bathrellos et al. 2009; Oh et al. 2011; Pradhan and Lee 2010; Intarawichian and Dasananda 2011). More recently, Shahabi evaluated three LSM models (Shahabi et al. 2014): the analytical hierarchy process, the frequency ratio, and the logistic regression models. Nourani compared susceptibility maps with results from previous analyses by adopting frequency ratio, LR, and artificial neural network models (Nourani et al. 2014). Che presented a comparative study of seed cells, InV, and generalized linear regression procedures for LSM (Che et al. 2012). A number of other statistical techniques for predicting LSM have been evaluated by other researchers (Rozos et al. 2011, 2013; Devkota et al. 2013; Kayastha et al. 2013; Ozdemir and Altural 2013; Pourghasemi et al. 2013, 2014; Pradhan 2013; Regmi et al. 2014).

The literature mentioned above covers numerous studies that apply the InV and LR methods for LSM. Despite the popularity of these two methods, their efficacy has yet to be comparatively assessed when the methods are employed for landslide mapping; they were previously employed separately in landslide susceptibility studies.

This paper applies the InV and LR methods to the same study area and compares the results for the first time. The objective of this study was to access and compare the performance of the InV and FR models and provide a detailed landslide susceptibility analysis of the Three George Reservoir area.

Description of the study area

The Three Gorges lie in the mountains separating the Sichuan and Jiangnan Basins along the middle reaches of the Yangtze River. In response to episodic tectonic uplift during the Quaternary Period, the gorges were formed by river incisions into the massive limestone mountains of the Early Paleozoic to Mesozoic Eras (J1 Jialinjiang Group) (Chen et al. 1995; Li et al. 2001). The elevation ranges from 800 to 2000 m. The terrain consists of a succession of limestone ridges and gorges with intergorge valleys comprised primarily of interbedded mudstone, shale, and thinly bedded limestone. Landslides tend to occur in failure-prone lithological formations that are concentrated in the intergorge valleys (Fourniadis et al. 2007).

The study area is located in Hubei Province, which includes Zigui and Badong counties, to the west of the Xiling Gorge (Fig. 1). The site lies between latitudes of 30.02°N and 30.93°N and longitudes of 110.30°E and 110.87°E and covers an area of 396 km². The geomorphology of the area is characterized by a rugged topography with hill ranges varying from 800 to 2000 m. The Yangtze River broadly crosses the study area in a WNW–ESE direction. The climate in the area is typically subtropical and monsoonal, with hot and humid summers but cold and dry winters. The average annual precipitation is 1100 mm. The rainfall is generally concentrated in spring and summer, and the summer average can be as high as 200–300 mm per month (He et al. 2008).

The geological base of the study area is composed of crystalline, pre-Sinian rocks with a Sinian–Jurassic sedimentary cover (Wu et al. 2001). The Huangling anticline to the northeast of Zigui county forms a structure of approximately 73 km in length, primarily oriented NNE–SSW, and its core consists of pre-Sinian metamorphic and magmatic rocks (Fig. 2).

Materials and methods

Landslide inventory

Landslides were identified based on the interpretation of 1:10,000-scale color aerial photographs. A series of field surveys were conducted to confirm the sizes and shapes of the landslides, define the types of movements and the materials involved, and review historical and bibliographical data, including geological, geomorphologic, and landslide maps. A total of 202 landslides were mapped and subsequently digitized and rasterized in ESRI's ArcGIS software with a grid cell size of 28.5 × 28.5 m. The grid size reflects the resolution of the digital elevation model (DEM) and the remote sensing data used. Other vector data layers, such as bedding structure and lithology, were also rasterized with this grid size. The study area was divided into 549,127 mapping units (grid cells), including 28,717 cells for landslides. The mapped landslides covered an area of 23.33 km², representing 5.23 % of the study area. The smallest landslide that could be identified from the aerial photographs and subsequently recognized in the field had an area of 0.0021 km², whereas the largest landslide, the Fanjiaping landslide located on the southern side of the Yangtze River, was approximately 1.5 km².

Landslide causative factors

Several researchers have examined the correlations between natural landslide occurrences in the Three Gorges

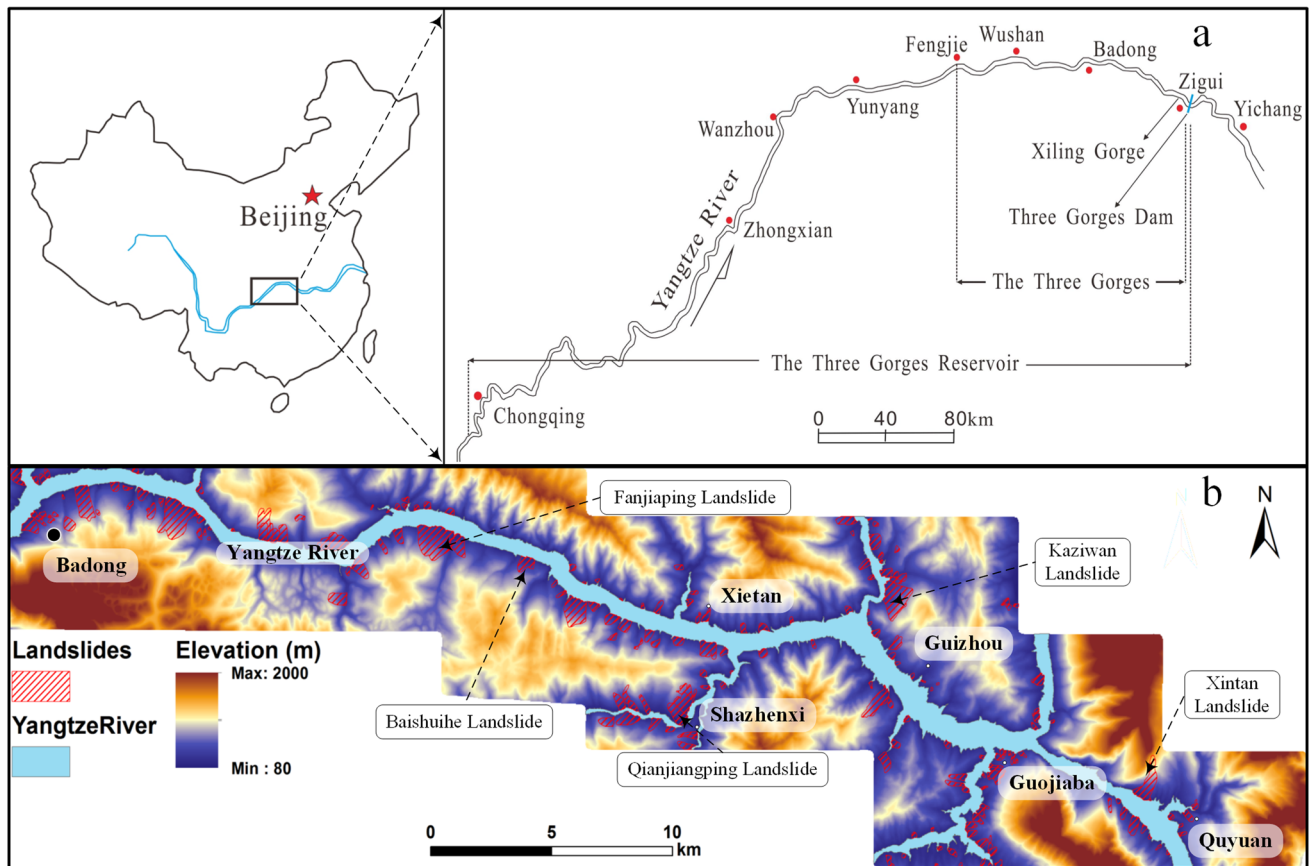


Fig. 1 Location map of the study area. **a** Sitemap of the Three Gorges area of the Yangtze River, China. **b** Digital elevation model (DEM) overlaid with landslides

area and various parameters such as elevation, slope angle, slope aspect, curvature, land cover, lithology, bedding structure, and lineaments based on remote sensing and GIS data (Bai et al. 2010; Fourniadis et al. 2007; Liu et al. 2004).

Based on previous research (Bai et al. 2010; Fourniadis et al. 2007; Peng et al. 2014; Liu et al. 2004) and our field reconnaissance, a total of 8 causative factors were considered in this study: lithology, bed rock–slope relationship, slope, aspect, elevation, profile curvature, plan curvature, and fractional vegetation cover. The continuous variables were converted into four classes by using the natural breaks method in the ArcGIS V9.3 software platform. The details of each factor are presented below.

Lithology

As a part of geomorphologic studies, the landslide phenomenon is related to the lithology of the land. Because different lithological units have different landslide susceptibility values, they are important in providing data for susceptibility studies; it is therefore essential to properly

group lithological properties (Dai et al. 2001; Duman et al. 2006). The geological map of the study area was prepared by the Hubei Province Geological Survey (HPGS) at a 1:50,000 scale and digitized in GIS (Hubei Province Geological Survey 1997). The study area possesses various types of lithological units. The lithology map of the area is shown in Fig. 3.

Bedding structure

Geological structures exert a strong influence on slope stability because different degrees of landsliding relate to the angular relationships between bedding attitudes, slope aspects, and slope angles (Meentemeyer and Moody 2000; Wen et al. 2004; Wu et al. 2004). When a bedding plane appears on a slope’s free face, a relatively stable condition can be presumed if the dip angle is greater than the slope angle; an unstable setting is formed if the dip angle is less than the slope angle. Geological structures provide a primary control on the position of slippery surfaces, and in the majority of landslides in the Three Gorges area, the failure surfaces were closely associated with a pre-existing planes of weakness (Wu et al. 2001).

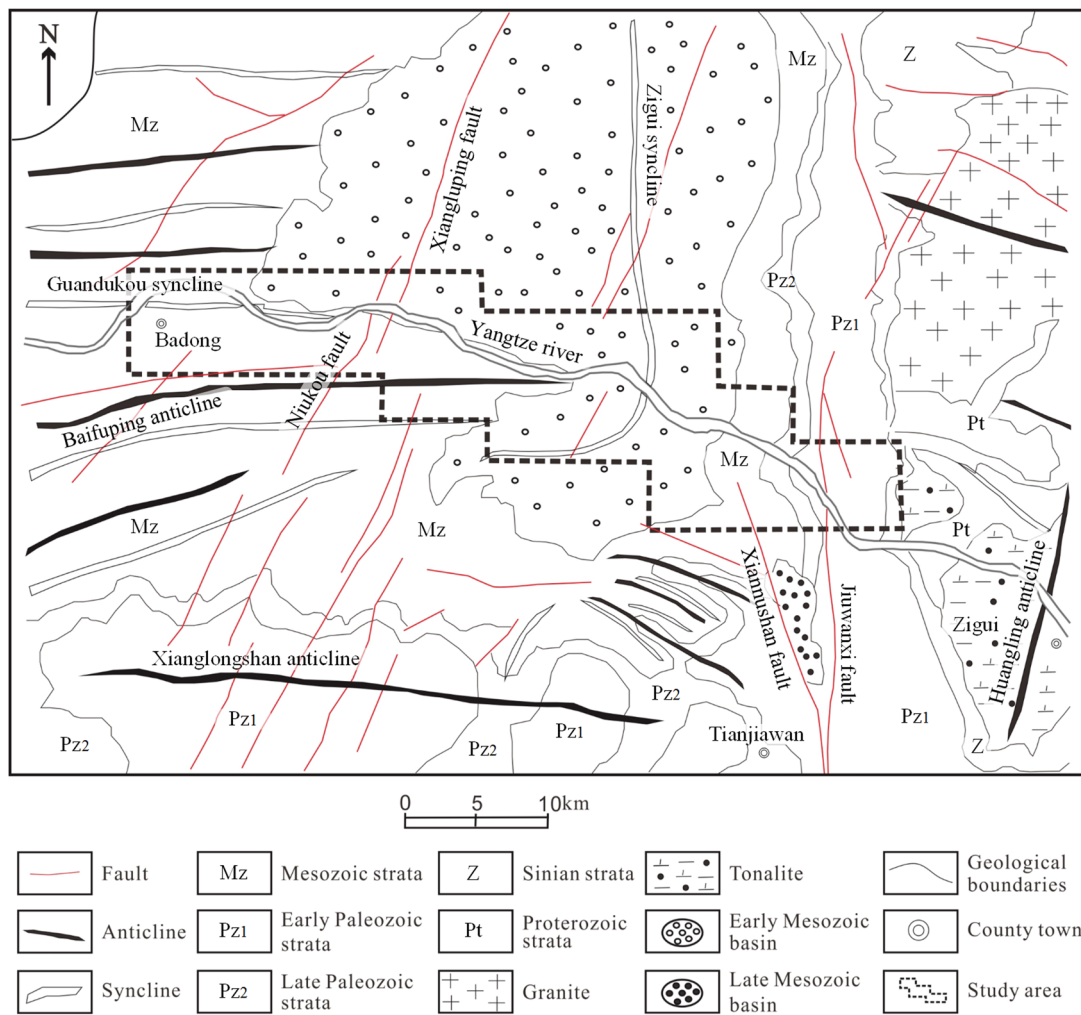


Fig. 2 Regional geological and tectonic framework map of the study area (Peng et al. 2014)

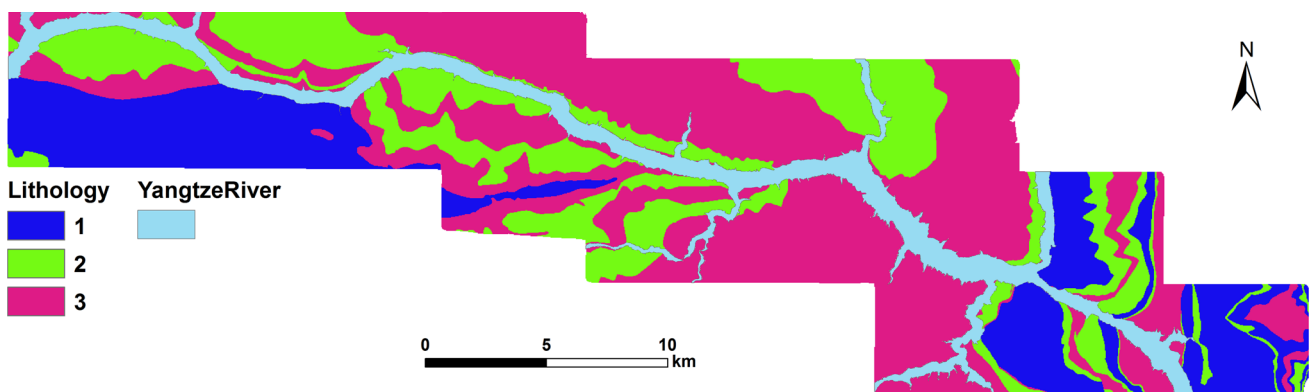


Fig. 3 Lithology map of the study area. (1 mudstone, shale, and Quaternary deposits, 2 sandstones and thinly bedded limestones, 3 limestones and massive sandstones)

Bedding structure can be classified as over-dip slopes, under-dip slopes, dip-oblique slopes, transverse slopes, anacinal-oblique slopes, and anacinal slopes. The relationship

between the bed dip direction and angle, as well as information on the slope angle and aspect, is shown in Table 1. These data were used to generate the bedding structure map (Fig. 4)

Table 1 Classification of the bedding structure relationship

Type	Definition
Over-dip slopes	$ \alpha - \beta \in [0^\circ, 30^\circ)$ or $ \alpha - \beta \in [330^\circ, 360^\circ)$, $\gamma > 10^\circ$ and $\delta > \gamma$
Under-dip slopes	$ \alpha - \beta \in [0^\circ, 30^\circ)$ or $ \alpha - \beta \in [330^\circ, 360^\circ)$, $\gamma > 10^\circ$ and $\delta < \gamma$
Dip-oblique slopes	$ \alpha - \beta \in [30^\circ, 60^\circ)$ or $ \alpha - \beta \in [300^\circ, 330^\circ)$
Transverse slopes	$ \alpha - \beta \in [60^\circ, 120^\circ)$ or $ \alpha - \beta \in [240^\circ, 300^\circ)$
Anaclinal-oblique slopes	$ \alpha - \beta \in [120^\circ, 150^\circ)$ or $ \alpha - \beta \in [210^\circ, 240^\circ)$
Anaclinal slopes	$ \alpha - \beta \in [150^\circ, 210^\circ)$

α is the slope aspect, β is the bed dip direction, γ is the bed dip angle, and δ is the slope angle

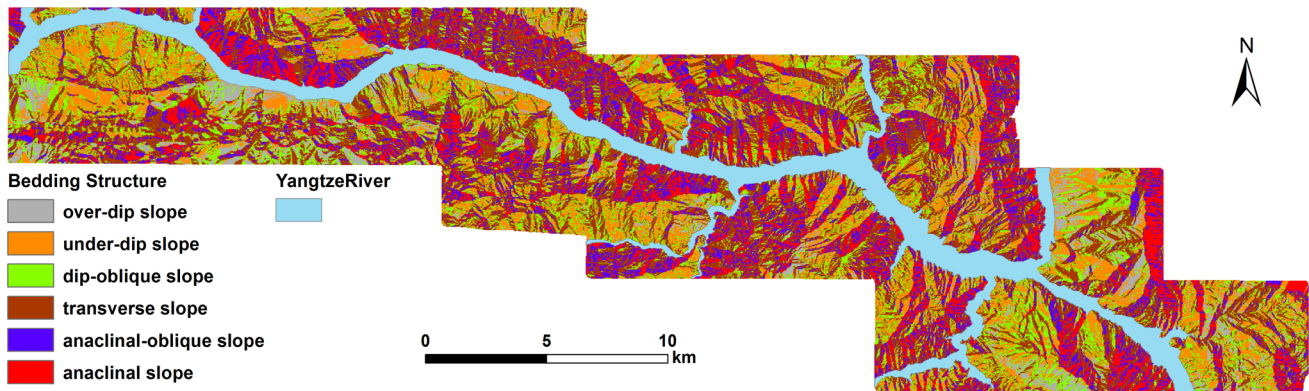


Fig. 4 Bedding structure map of the study area

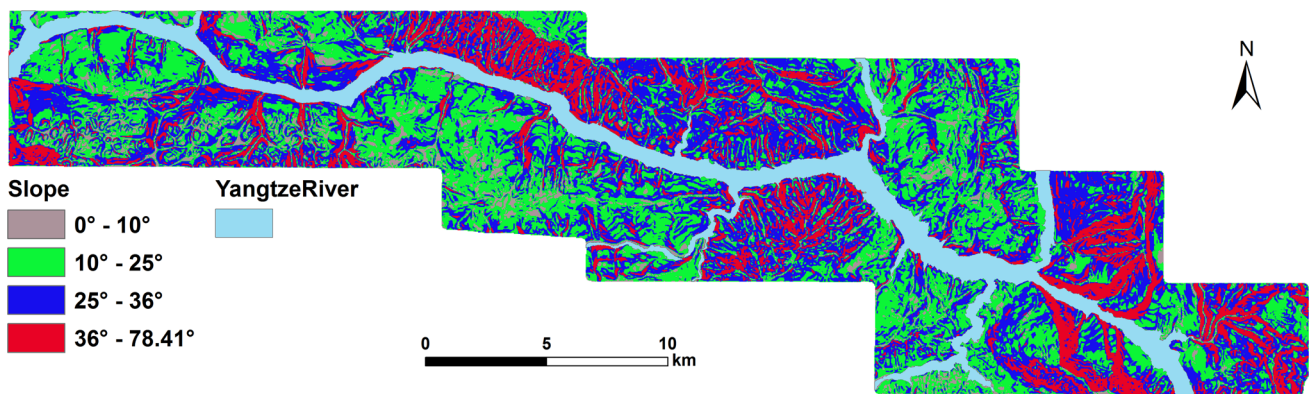


Fig. 5 Slope map of the study area

Slope

The slope angle is a major parameter in landslide susceptibility mapping because it is directly related to landslides (Lee and Min 2001; Cevik and Topal 2003; Lee et al. 2004). The slope map was derived from DEM with a 30×30 m grid size. The original slope angles vary between 0° and 78.41° , and the values were reclassified into 4 categories: (1) 0° to 10° , (2) 10° to 25° , (3) 25° to 36° , and (4) 36° to 78.41° (Fig. 5).

Aspect

Similar to slope, aspect is also a major factor in landslide susceptibility mapping (Guzzetti et al. 1999; Cevik and Topal 2003; Lee et al. 2004). In this study, the aspect of the study area was classified as flat (-1°), north (0° – 22.5° and 337.5° – 360°), northeast (22.5° – 67.5°), east (67.5° – 112.5°), southeast (112.5° – 157.5°), south (157.5° – 202.5°), southwest (202.5° – 247.5°), west (247.5° – 292.5°), and northwest (292.5° – 337.5°) (Fig. 6).

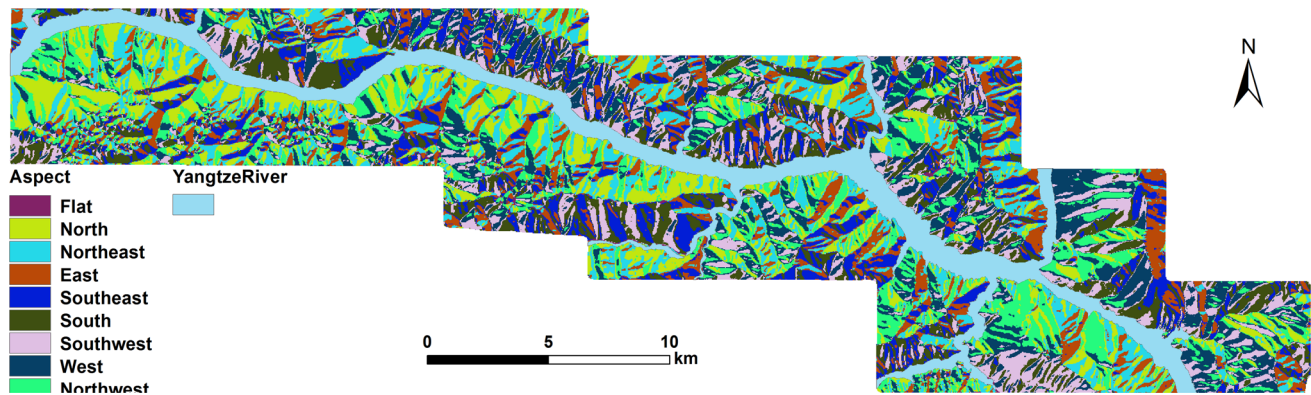


Fig. 6 Aspect map of the study area

Elevation

Elevation is also a relevant landslide conditioning factor used in this study. The elevation map was prepared from 1:10,000-scale digital topographic maps surveyed by Three Gorges Headquarters with a spatial resolution of 28.5 m. The original elevations vary between 80 and 2000 m and are grouped into four classes: (1) 80–330 m, (2) 330–620 m, (3) 620–1000 m, and (4) 1000–2000 m (Fig. 7).

Profile curvature

The profile curvature is the curvature that corresponds to a normal section that is tangential to a flow line; it shows the flow acceleration and erosion/deposition (negative values/positive values) rate while providing a basic indication of geomorphology (Yesilnacar, and Topal 2005). In addition, the profile curvature controls the change of velocity of mass flowing down the slope (Talebi et al. 2007). A profile curvature map was produced with the original profile curvature values varying between $-33.47^{\circ}/100$ m and $31.99^{\circ}/$

100 m, and the values were reclassified into four classes: (1) -33.47 to $-1.123^{\circ}/100$ m, (2) -1.123 to $0.161^{\circ}/100$ m, (3) 0.161 to $1.702^{\circ}/100$ m, and (4) 1.702 to $31.99^{\circ}/100$ m (Fig. 8).

Plan curvature

The term curvature is theoretically defined as the rate of change of slope gradient or aspect, typically in a particular direction (Wilson and Gallant 2000). The curvature value can be evaluated by calculating the reciprocal value of the radius of curvature of a particular direction (Nefeslioglu et al. 2008). Thus, whereas the curvature values of broad curves are small, tight curves have higher values. For this reason, this parameter constitutes one of the conditioning factors controlling landslide occurrences. A plan curvature map was produced with original plan curvature values varying between $-11.96^{\circ}/100$ m and $17.04^{\circ}/100$ m, and the values were reclassified into four classes: (1) -11.96 to $-1.497^{\circ}/100$ m, (2) -1.497 to $-0.360^{\circ}/100$ m, (3) -0.360 to $0.437^{\circ}/100$ m, and (4) 0.437 to $17.04^{\circ}/100$ m (Fig. 9).

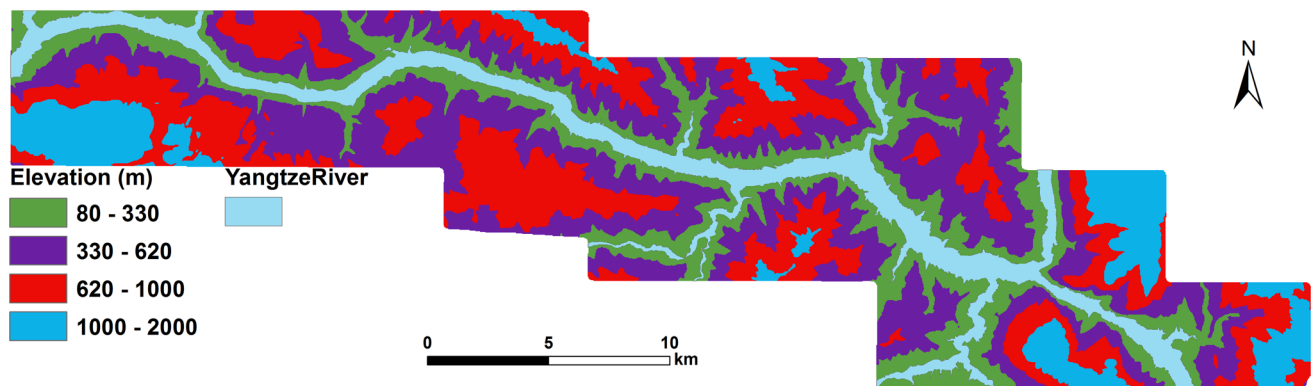


Fig. 7 Elevation map of the study area

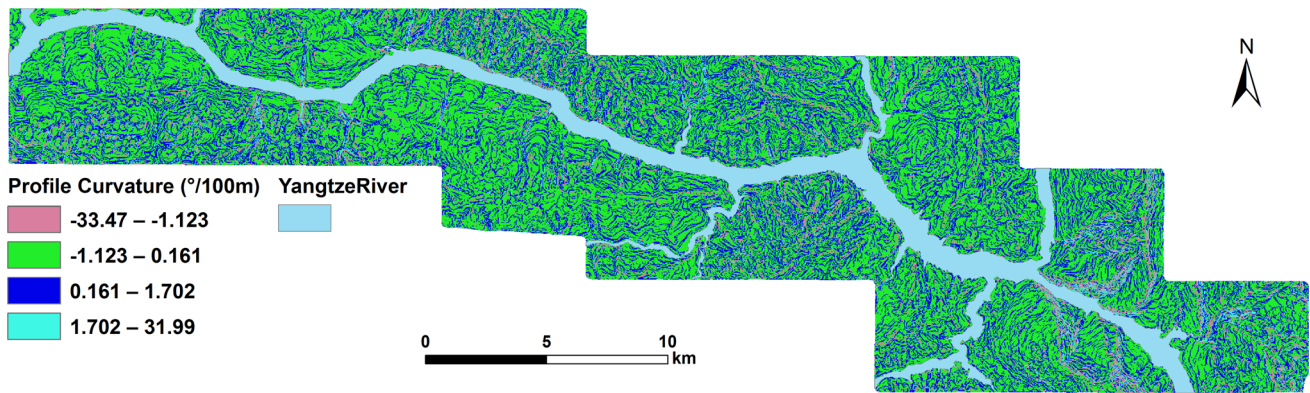


Fig. 8 Profile curvature map of the study area

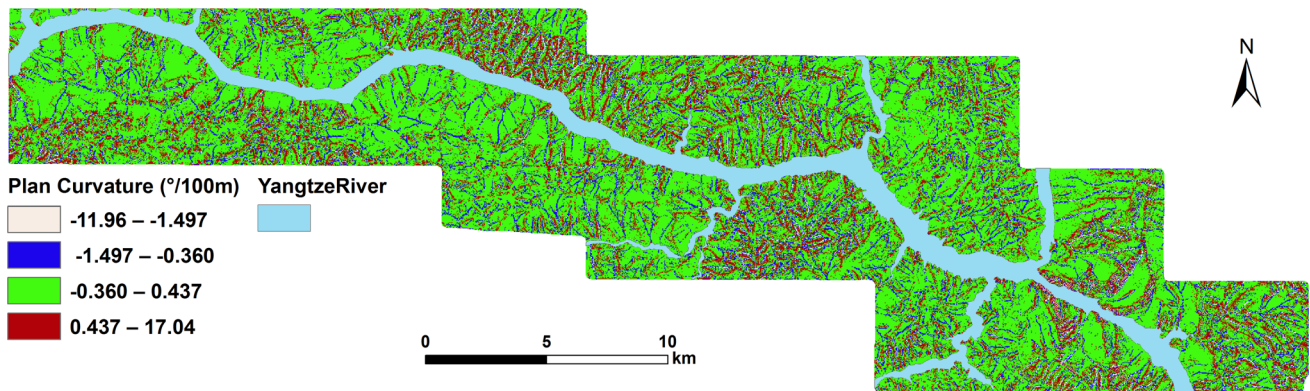


Fig. 9 Plan curvature map of the study area

Fractional vegetation cover

Fractional vegetation cover (FVC) is an important factor influencing the occurrence and movement of landslides because changes in the FVC often result in modified landslide behavior (Glade 2003; Chen et al. 2009). The FVC can reduce the frequency of landslides due to the vegetation canopy and ground cover, but it is one of the most difficult

parameters to estimate over broad geographical areas. In this paper, the FVC was calculated from CBERS (China-Brazil Earth Resources Satellite) data acquired in April 2004 with a path/row of 04/65. The calculation was performed using a back-propagation neural network (BPNN) (Chen et al. 2011a, b). A fractional vegetation cover map was produced and reclassified into four classes: (1) 0–16 %, (2) 16–35 %, (3) 35–60 %, and (4) 60–100 % (Fig. 10).

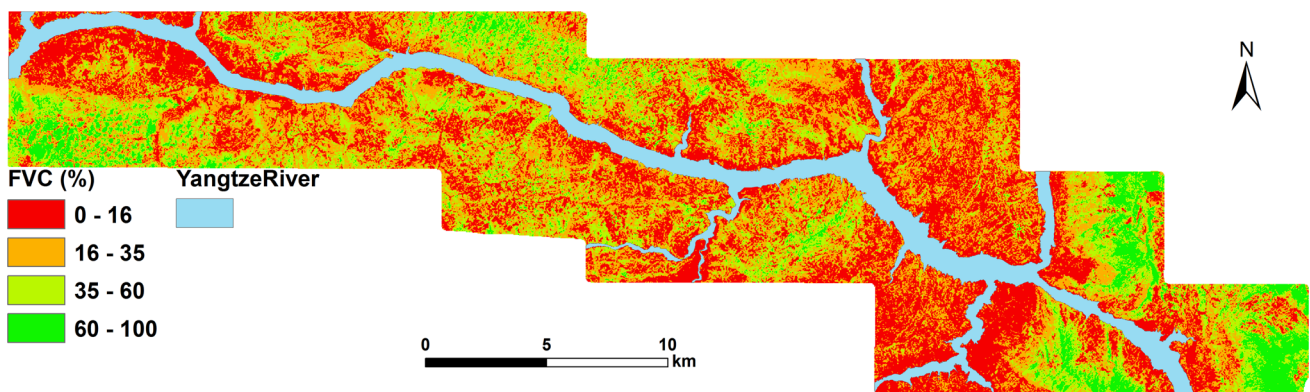


Fig. 10 Fractional vegetation cover map of the study area

Methodology

Information value model

The information value (InV) method involves the selection of a set of instability factors. The information value I_i of each causative factor X_i is determined by Yin and Yan (1988)

$$I_i = \log \frac{S_i/N_i}{S/N} \quad (1)$$

where S_i is the number of landslide pixels with the presence of causative factor X_i , N_i is the number of pixels with causative factor X_i , S is the total number of landslide pixels, and N is the total number of pixels in the study area.

A negative value of I_i indicates that the presence of a certain causative factor is irrelevant in landslide development. A positive value of I_i indicates a relevant relationship between the presence of a certain causative factor and landslide distribution. The stronger the relationship, the higher the score (Yan 1988).

The total information value I can then be obtained by

$$I = \sum_{i=1}^n \log \frac{S_i/N_i}{S/N} \quad (2)$$

The InV method is an indirect statistical approach that has the advantage of assessing landslide susceptibility in an objective way. The method allows for a quantified prediction of susceptibility by means of a score, even on terrain units not yet affected by a landslide. Each causative factor is crossed with the landslide distribution; as with all bivariate statistical methods, weighted values based on landslide densities are calculated for each parameter class. The correlations between the input variables are not accounted for.

Logistic regression model

To indicate the presence and absence of a landslide in the logistic regression (LR) method, the dependent variable is coded as “1” and “0,” respectively. The logistic model representing the maximum likelihood regression model can be expressed in its simplest form as follows:

$$P = \frac{1}{1 + e^{-z}} \quad (3)$$

where P is the probability of event (landslide) occurrence, which varies from 0 to 1 on an s-shaped curve and is defined as the landslide susceptibility index (LSI) in this paper. The parameter z is defined in the following equation (linear logistic model) with values between $-\infty$ and $+\infty$:

$$z = B_0 + B_1X_1 + B_2X_2 + \dots + B_nX_n \quad (4)$$

where B_0 is the intercept of the model and n is the number of independent variables. The parameter B_i ($i = 0, 1, 2, \dots$,

n) represents the slope coefficients of the logistic regression model, and X_i ($i = 0, 1, 2, \dots, n$) represents the independent variables. The linear model formed is a logistic regression representing the presence or absence of landslides (under present conditions) with respect to the independent variables (pre-failure conditions).

Based on Eqs. (3) and (4), the logistic regression equation can be written in the following extended form:

$$P = \frac{1}{1 + e^{-B_0 + B_1X_1 + B_2X_2 + \dots + B_nX_n}} \quad (5)$$

Logistic regression is useful in predicting the presence or absence of a characteristic because it allows for the creation of a multivariate regression relation between a dependent variable and several independent variables (Atkinson and Massari 1998; Süzen and Doyuran 2004; Hosmer and Lomeshow 2000; Süzen 2002; Lee 2005). The coefficients determined in LR can be used to estimate the ratios for each of the independent variables.

Results and discussion

Application of information value model

To understand the determinants of the landslide, the information value of the each possible factor responsible for the landslide was computed by the information value method (Table 2). The final landslide susceptibility map obtained by the InV model is shown in Fig. 11.

The majority of landslides occurred in sandstone and thinly bedded limestone with an information value of 0.27 and contained within 51.67 % of the landslide area. Limestone and massive sandstones have a low contribution to landslide occurrences (-0.034 of information value within 44.82 % of landslide area), whereas mudstone, shale, and Quaternary deposits have the lowest contribution to landslide occurrences (-0.834 of information value with 3.51 % of landslide area) among these three lithology categories.

Bedding structure is an important causative factor representing the angular relationship between topography and strata attitude. The maximum information value of bedding structure was 0.107, and the minimum was -0.401 in the study area. This implies that under-dip slopes have a higher possibility of landslide occurrence with 22.84 % of the landslide area, whereas over-dip slopes have the lowest possibility of landslide occurrence because they contain 2.54 % of the landslide area.

The information values of slope vary from -0.650 to 0.226. In the study area, approximately 62.5 % of the landslides occurred below 25° . Over half of the landslides (58.4 %) occurred between slopes of 10° – 25° . Overall, no definite correlation was found between slope angle and

Table 2 Information values calculated for each categories of causative factors, based on information value method; coverage area, and area of the existing landslides in that category

Causative factors	Categories	S_i	N_i	S_i/N_i	Area (%)	Landslides area (%)	Information value
Lithology	Mudstone, shale, and Quaternary deposits	1008	131,507	0.00766	23.95	3.51	-0.834
	Sandstones and thinly bedded limestones	14,837	150,992	0.982635	27.50	51.67	0.274
	Limestones and massive sandstones	12,872	266,628	0.48277	48.55	44.82	-0.034
Bedding structure	Over-dip slopes	730	35,127	0.020782	6.40	2.54	-0.401
	Under-dip slopes	6558	98,011	0.066911	17.85	22.84	0.107
	Dip-oblique slopes	5631	95,195	0.059152	17.34	19.61	0.054
	Transverse slopes	8657	159,290	0.054347	29.01	30.15	0.017
	Anaclinal-oblique slopes	3985	81,919	0.048646	14.92	13.88	-0.031
	Anaclinal slopes	3156	79,584	0.039656	14.49	10.99	-0.120
Slope (°)	0–10	1184	65,613	0.018045	11.95	4.12	-0.462
	10–25	16,773	190,708	0.087951	34.73	58.41	0.226
	25–36	9724	204,244	0.047610	37.19	33.86	-0.041
	36–78.41	1036	88,562	0.011698	16.13	3.61	-0.650
Aspect	Flat	0	34,817	0.000000	6.34	0.00	0.000
	North	6507	73,443	0.088599	13.37	22.66	0.229
	Northeast	4999	70,594	0.070813	12.86	17.41	0.132
	East	2719	56,438	0.048177	10.28	9.47	-0.036
	Southeast	2270	57,374	0.039565	10.45	7.90	-0.121
	South	3855	62,089	0.062088	11.31	13.42	0.075
	Southwest	1881	60,571	0.031054	11.03	6.55	-0.226
	West	2283	70,368	0.032444	12.81	7.95	-0.207
Elevation (m)	80–330	4203	63,433	0.066259	11.55	14.64	0.103
	330–620	20,510	170,890	0.120019	31.12	71.42	0.361
	620–1000	7842	186,406	0.042069	33.95	27.31	-0.094
	1000–2000	365	134,329	0.002717	24.46	1.27	-1.284
Profile curvature (°/100 m)	0	0	57,502	0.000000	10.47	0.00	0.000
	-33.47 to -1.123	563	32,286	0.017438	5.88	1.96	-0.477
	-1.123 to 0.161	20,060	337,061	0.059514	61.38	69.85	0.056
	0.161 to 1.702	7817	161,237	0.048481	29.36	27.22	-0.033
Plan curvature (°/100 m)	1.702 to 31.99	277	18,543	0.014938	3.38	0.96	-0.544
	-11.96 to -1.497	191	12,031	0.015876	2.19	0.67	-0.518
	-1.497 to -0.360	2987	67,314	0.044374	12.26	10.40	-0.071
	-0.360 to 0.437	23,875	387,014	0.061690	70.48	83.14	0.072
Fractional vegetation cover (%)	0.437 to 17.04	1664	82,768	0.020104	15.07	5.79	-0.415
	0–16	17,883	232,230	0.077006	42.29	62.27	0.168
	16–35	8971	179,666	0.049932	32.72	31.24	-0.020
	35–60	1746	101,028	0.017282	18.40	6.08	-0.481
	60–100	117	36,203	0.003232	6.59	0.41	-1.209

landslide occurrence, although the relationship was positive for slopes up to 36°.

Among the aspect categories, the maximum information value was found on the north-facing slope (0.229) and the minimum on the southwest faces (-0.226). Therefore, the

maximum number of landslides was concentrated in the north and northeast slope directions.

As for the elevation factors, more than two-thirds (71.42 %) of the landslides occurred within 330 m of elevation. Beyond this height, the occurrence of landslides

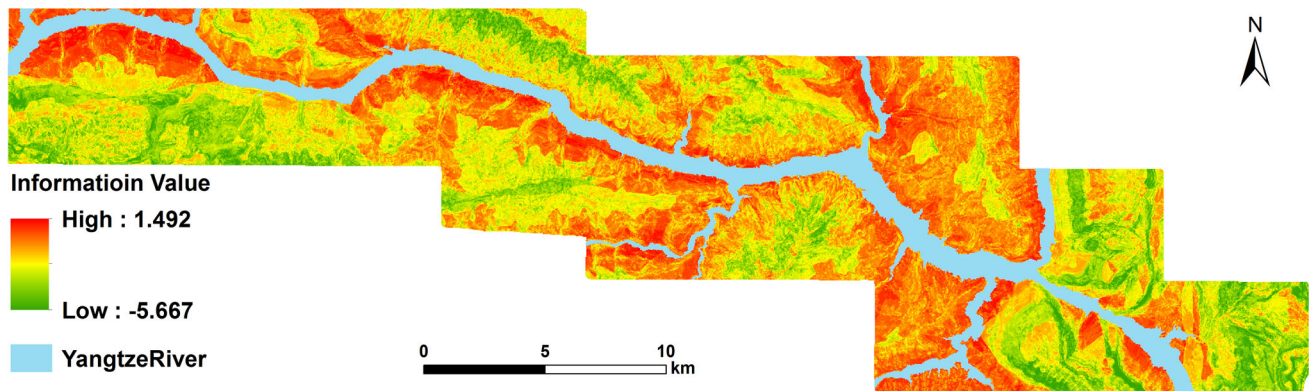


Fig. 11 Landslide susceptibility maps obtained from InV model

gradually decreases, and the elevation factors have insignificant contributions beyond 620 m.

The profile curvature and plan curvature factors play similar roles. The highest information value of profile curvature categories was 0.056 and occurred between -1.123 and 0.161 ($^{\circ}/100$ m), whereas one of the plan curvature categories was 0.072 and occurred between -0.360 and 0.437 ($^{\circ}/100$ m).

In this study, fractional vegetation cover was negatively correlated with landslide occurrences. The highest rating was found where fractional vegetation cover was $<16\%$ and the influence was negligible for vegetation cover $>80\%$.

Application of logistic regression model

The LR analysis method and GIS techniques were employed in this study to extract an evaluation of LS in the study area. Eight landslide causative factors were considered and described in the previous section.

The landslide causative factors used in this study are also displayed in Table 2. Experts in the field generally recommend that researchers use approximately equal proportions of landslide-present (1) and landslide-absent (0) pixels in LR (Ayalew and Yamagishi 2005); this analysis features 4808 landslide-present pixels and 4800 randomly selected landslide-absent pixels. The 4808 landslide occurrence cells account for 0.5 % of the total study area. The class values of the dependent (landslide-present and landslide-absent points) and independent variables (landslide causative factors) were determined at 9608 points to create the input table for LR modeling. The model coefficients were estimated using the statistical analysis software SPSS V22.0 (Table 3). Based on the obtained results, Eq. (4) can be rewritten as follows:

$$z = L_c + BS_c + A_c - 4.127 \times S - 16.316 \times E - 0.247 \times PrC + 0.226 \times PIC - 1.875 \times FVC + 3.786 \quad (6)$$

where L_c , BS_c , and A_c are the logistic regression coefficient values listed in Table 3; S is the slope value; E is the elevation value; PrC is the profile curvature value; PIC is the plan curvature value; and FVC is the fractional vegetation cover value.

Finally, the landslide susceptibility index (LSI) map is obtained by using the raster calculator in ArcGIS 9.3 and is based on Eq. (5) (Fig. 12).

It can be observed in Table 3 that plan curvature plays a prominent role in the landslide susceptibility of the area because it has a positive B value (0.226). The slope, elevation, profile curvature, and fractional vegetation cover have a negative effect in landslide formation because they all have a negative B coefficient. As for lithology, the limestone and massive sandstone deposits ($B = 0.861$) are the most susceptible to sliding. The mudstone, shale, and Quaternary deposits ($b = -0.020$), along with the sandstone and thinly bedded limestone (-0.822), have negative B coefficients and are thus less susceptible to landslides. As for the bedding structure, the transverse slopes ($b = 0.425$), dip-oblique slopes ($b = 0.410$), anacinal slopes ($b = 0.339$), anacinal-oblique slopes ($b = 0.316$), and under-dip slopes ($b = 0.029$) have a high probability of landslide susceptibility as they have a positive b coefficient, while over-dip slopes ($b = -0.680$) have less probability because they have a negative B coefficient. As for aspect, the slopes trending toward the southeast ($b = 0.397$), northeast ($b = 0.350$), and east ($b = 0.077$) have susceptibility levels in decreasing order, whereas the remaining aspect categories play a negative role in the landslide susceptibility of the region.

Table 3 Coefficient of logistic regression model

Causative factors	Categories	<i>B</i> ^a	S.E. ^b	Wald ^c	Df ^d	Sig. ^e	Exp(B) ^f
Lithology (<i>L_C</i>)	Mudstone, shale, and Quaternary deposits	-0.020	0.496	0.002	1	0.967	0.980
	Sandstones and thinly bedded limestones	-0.822	0.120	47.175	1	0.000	0.439
	Limestones and massive sandstones	0.861	0.064	182.968	1	0.000	2.365
Bedding structure (<i>BS_C</i>)	Over-dip slopes	-0.680	0.453	2.255	1	0.133	0.507
	Under-dip slopes	0.029	0.184	0.024	1	0.876	1.029
	Dip-oblique slopes	0.410	0.107	14.595	1	0.000	1.507
	Transverse slopes	0.425	0.108	15.345	1	0.000	1.529
	Anaclinal-oblique slopes	0.316	0.098	10.412	1	0.001	1.371
	Anaclinal slopes	0.339	0.111	9.298	1	0.002	1.404
	Slope (<i>S</i>)		-4.127	0.285	209.197	1	0.000
Aspect (<i>A_C</i>)	Flat	-3.166	0.624	25.720	1	0.000	0.042
	North	-3.416	1.332	6.576	1	0.010	0.033
	Northeast	0.350	0.103	11.653	1	0.001	1.419
	East	0.077	0.105	0.545	1	0.461	1.081
	Southeast	-0.099	0.114	0.760	1	0.383	0.906
	South	-0.511	0.121	17.942	1	0.000	0.600
	Southwest	0.397	0.113	12.454	1	0.000	1.488
	West	-0.923	0.124	55.487	1	0.000	0.397
	Northwest	-0.597	0.116	26.729	1	0.000	0.550
Elevation (<i>E</i>)		-16.316	0.405	1627.088	1	0.000	0.000
Profile curvature (PrC)		-0.247	1.658	0.022	1	0.882	0.781
Plan curvature (PIC)		0.226	2.088	0.012	1	0.914	1.253
Fractional vegetation cover (FVC)		-1.875	0.229	66.924	1	0.000	0.153
Constant		3.786	1.273	8.846	1	0.003	44.097

^a *B* = logistic coefficient

^b S.E. = standard error of estimate

^c Wald = Wald Chi-square values

^d Df = degree of freedom

^e Sig. = Significance

^f Exp(B) = exponentiated coefficient

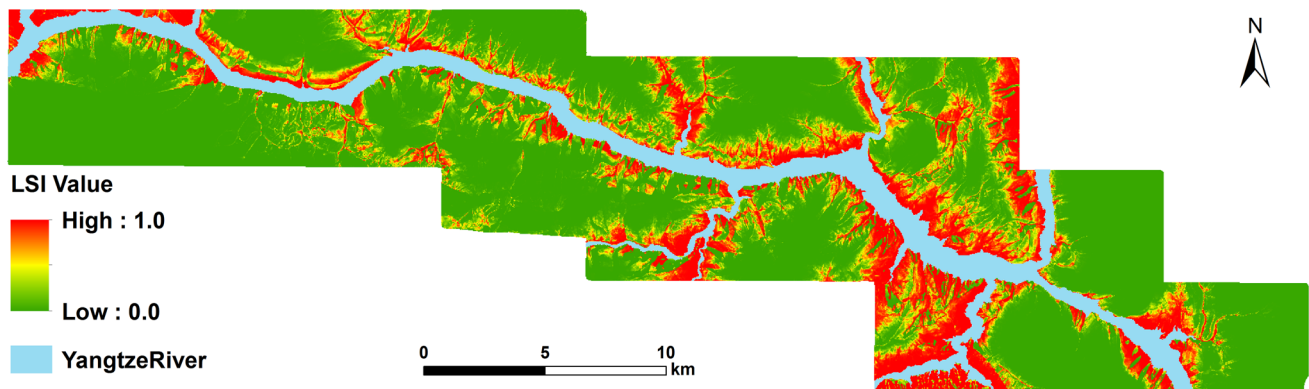


Fig. 12 Landslide susceptibility maps obtained from LR model

Validation of the landslide susceptibility maps

The values obtained from the InV and LR models range from -5.667 to 1.492 and 0 to 0.9991 , respectively. The mean and standard deviation values in the two LSMs obtained from the InV and LR models are -0.7387 , 1.1498 , 0.1356 , and 0.3595 , respectively. To improve the readability of the map, the natural breaks method in ArcGIS was used to divide the two probability maps into four susceptibility zones: very low, low, medium, and high (Figs. 13, 14).

The results of the two LSMs were validated by comparing them with the existing landslide locations and using the success-rate and prediction-rate methods (Chung and Fabbri 2003). The success-rate results were obtained by comparing the pixels from the 4808 pixels of landslide locations and the 4800 pixels of randomly selected non-landslide locations with the two landslide susceptibility maps. The success-rate curves of the two LSMs obtained from the InV and LR models are shown in Fig. 15.

However, the success-rate method may not be suitable for assessing the prediction capacity of the landslide models (Brenning 2005). The prediction rate can explain

how well the landslide models and landslide conditioning factors predict landslides (Pradhan and Lee 2010; Chung and Fabbri 2003; Brenning 2005). Therefore, in this study, the prediction-rate results were obtained based on the comparison of the landslide grid cells from the 4808 pixels of landslide locations and the 4800 pixels of randomly selected non-landslide locations that were not used in the training phase with the two LSMs. Figure 16 shows the prediction-rate curve results of the two LSMs obtained from the InV and LR models.

The accuracy of these two susceptibility maps was checked by using receiver operating characteristics (ROC). The ROC curve is a useful method of representing the quality of deterministic and probabilistic detection and forecast systems (Swets 1988). It can be equivalently represented by plotting the fraction of true positives out of the positives versus the fraction of false positives out of the negatives for a binary classifier system, as its discrimination threshold is varied (Table 4). By tradition, the plot shows the false-positive rate (1-specificity) on the x-axis (Eq. 7) and the true-positive rate (the sensitivity or 1-the false negative rate) on the y-axis (Eq. 8).

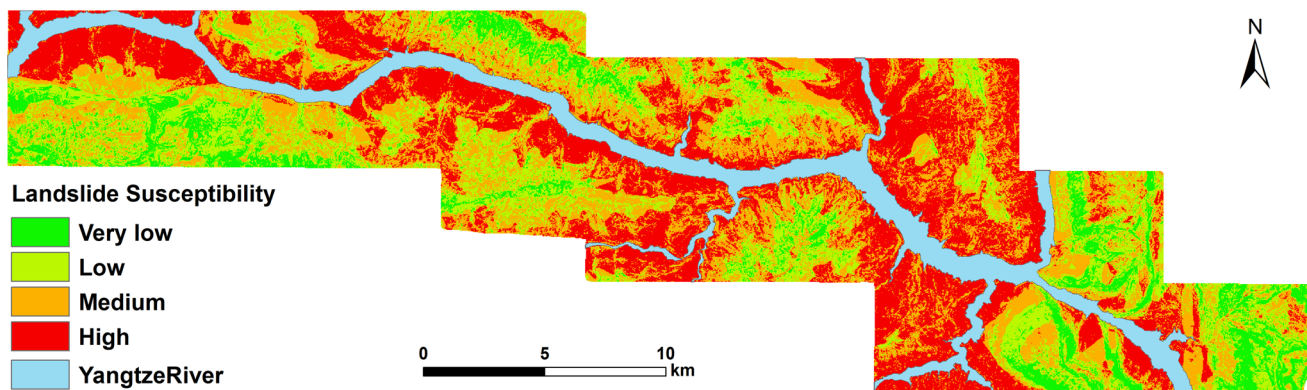


Fig. 13 Landslide susceptibility zone map obtained from InV model

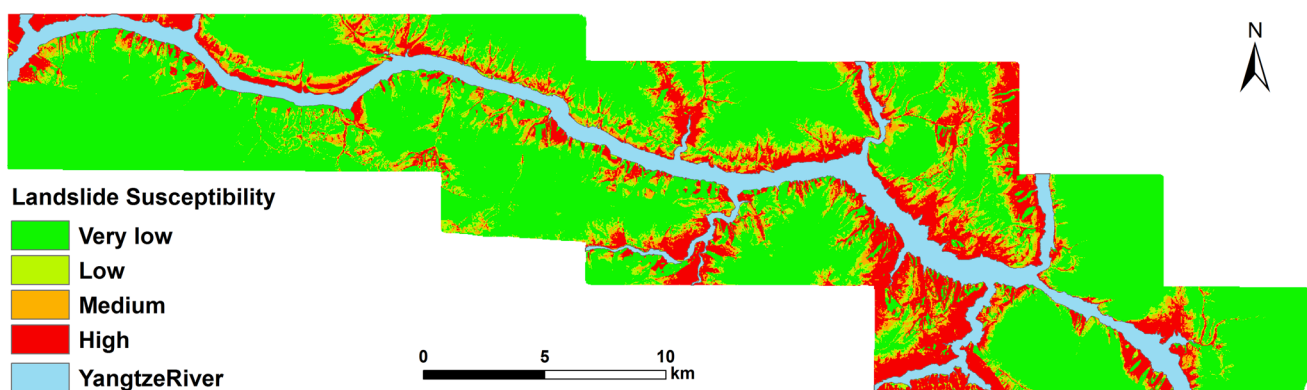


Fig. 14 Landslide susceptibility zone map obtained from LR model

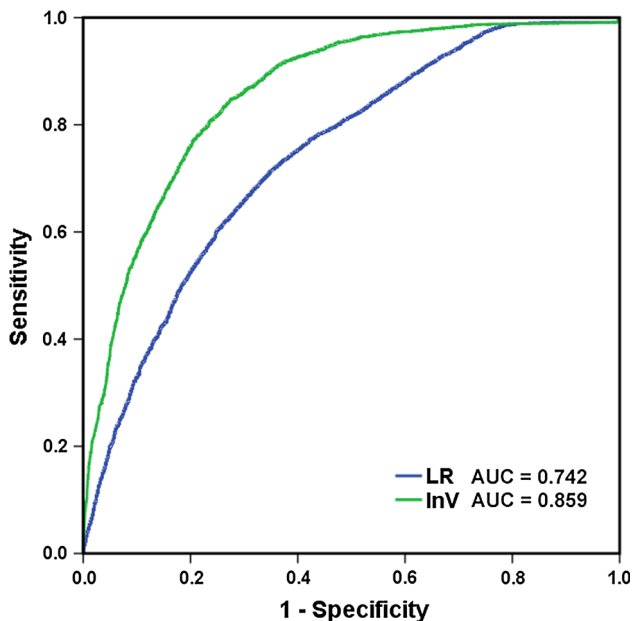


Fig. 15 Success-rate curve and areas under the curves (AUC) for the susceptibility maps produced by InV model and LR model in this study

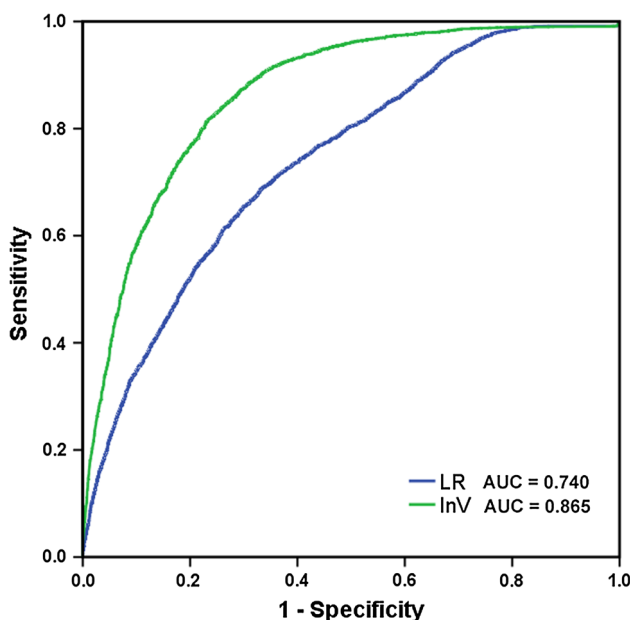


Fig. 16 Prediction-rate curve and areas under the curves (AUC) for the susceptibility maps produced by InV model and LR model in this study

Table 4 Parameters for the calculation of ROC curve (modified from Swets 1988)

	Landslide locations	Non-landslide locations
Landslide occurrence based on calculated function	True positive (TP)	False positive (FP)
Safe areas based on calculated function	False negative (FN)	True negative (TN)

$$X = 1 - \text{specificity} = 1 - \left[\frac{TN}{TN + FP} \right] \tag{7}$$

$$Y = \text{Sensitivity} = \left[\frac{TP}{FN + TP} \right] \tag{8}$$

The area under the ROC curve (AUC) characterizes the quality of a forecast system by describing the system’s ability to correctly predict the occurrence or non-occurrence of predefined “events.” The model with a greater AUC is considered to be the best. If the area under the ROC curve (AUC) is close to 1, then the result of the test is excellent. Conversely, an AUC result closer to 0.5 indicates a fairer test result. Both the success rate and prediction rate of the models were used for assessing the prediction capability of the models.

When the ROC curves of these two methods were considered together, their overall performances are observed to be slightly different. According to the obtained AUC in Figs. 15 and 16, the InV model demonstrates slightly higher accuracy performance (0.859 in success rate and 0.865 in prediction rate, both with an estimated standard error of 0.004) than the LR model (0.742 in success and 0.740 in prediction rate, both with an estimated standard error of 0.005). These results indicate that the InV model is a relatively good method of determining LSM in the study area and is appropriate for LSM based on the 0.865 accuracy for this area in prediction performance.

Conclusions

Over the last three decades, regional landslide susceptibility assessment has been a pressing research topic because it is a difficult and nonlinear problem. Although some studies have individually applied the InV or LR methods to generate LSM, these methods had not been directly and quantitatively compared. In this study, the InV and LR methods were applied in the same study area, and their performances were compared.

The results of the two LSMs obtained from both models were validated by comparing them with the known landslide locations using the success-rate and prediction-rate methods. The suitability of each model was evaluated by the area under the ROC curve. The results showed that the two methods employed in the present study gave promising results with more than 70 (AUC) prediction performances.

The prediction rate was higher than the success rate for the InV model, whereas the success rate was higher than the prediction rate for the LR model. The success-rate and prediction-rate results produced by the InV and LR methods were 0.859, 0.742, 0.865, and 0.740, respectively. The comparison results of this study indicate that the InV model has the higher prediction accuracy for the study area. The input, calculation, and output processes of the InV are relatively simple and easy to understand, whereas the LR model requires a preliminary conversion of data. The results obtained in this study also showed that the InV model can be used as a simple tool for the assessment of LSM when a sufficient number of data are collected.

Landslide susceptibility maps obtained from InV and LR should be assessed carefully by a landslide expert to identify cases where the model is overtrained and the prediction results are misleading. The results obtained in this paper show that the models followed in the present study exhibit reasonably satisfactory performance. As a final conclusion, the analyzed results obtained from the study can aid planners and engineers in future development and land-use planning for the Zigui–Badong area of the Three Gorges Reservoir in China.

Acknowledgments This work was funded in part by the CRSRI Open Research Program (CKWV2013221/KY), in part by the Natural Science Foundation of Hubei Province (2012FFB06501), and in part by the National High Technology Research and Development Program of China (2012AA121303).

References

- Akgun A, Turk N (2010) Landslide susceptibility mapping for Ayvalik (Western Turkey) and its vicinity by multicriteria decision analysis. *Environ Earth Sci* 61(3):595–611
- Akgun A, Kincal C, Pradhan B (2011) Application of remote sensing data and GIS for landslide risk assessment as an environmental threat to Izmir city (west Turkey). *Environ Monit Assess* 184(9):5453–5470
- Atkinson PM, Massari R (1998) Generalized linear modeling of susceptibility to landsliding in the central Apennines, Italy. *Comput Geosci* 24(4):373–385
- Ayalew L, Yamagishi H (2005) The application of GIS-based logistic regression for landslide susceptibility mapping in the Kakuda-Yahiko Mountains, Central Japan. *Geomorphology* 65(1):15–31
- Bai SB, Wang J, Zhang FY, Pozdnoukhov A, Kanevski MF (2008) Prediction of landslide susceptibility using logistic regression: a case study in Bailongjiang River Basin, China. In: *Proceedings of the 4th international conference on natural computation*, Jinan, China, pp 25–27
- Bai SB, Wang J, Lu GN, Zhou PG, Hou SS, Xu SN (2009) GIS-based and data-driven bivariate landslide-susceptibility mapping in the Three Gorges Area, China. *Pedosphere* 19(1):14–20
- Bai SB, Wang J, Lu GN, Zhou PG, Hou SS, Xu SN (2010) GIS-based logistic regression for landslide susceptibility mapping of the Zhongxian segment in the Three Gorges area, China. *Geomorphology* 115(1):23–31
- Balasubramani K, Kumaraswamy K (2013) Application of geospatial technology and information value technique in landslide hazard zonation mapping: a case study of Giri Valley, Himachal Pradesh. *Disaster Adv* 6(1):38–47
- Bathrellos GD, Kalivas DP, Skilodimou HD (2009) GIS-based landslide susceptibility mapping models applied to natural and urban planning in Trikala, Central Greece. *Estud Geol* 65(1):49–65
- Bathrellos GD, Gaki-Papanastassiou K, Skilodimou HD, Papanastassiou D, Chousianitis KG (2012) Potential suitability for urban planning and industry development by using natural hazard maps and geological—geomorphological parameters. *Environ Earth Sci* 66(2):537–548
- Bathrellos GD, Gaki-Papanastassiou K, Skilodimou HD, Skianis GA, Chousianitis KG (2013) Assessment of rural community and agricultural development using geomorphological—geological factors and GIS in the Trikala prefecture (Central Greece). *Stoch Environ Res Risk Assess* 27(2):573–588
- Brabb EE (1991) The world landslide problem. *Episodes* 14(1):52–61
- Brenning A (2005) Spatial prediction models for landslide hazards: review, comparison and evaluation. *Nat Hazards Earth Syst Sci* 5(6):853–862
- Cevik K, Topal T (2003) GIS-based landslide susceptibility mapping for a problematic segment of the natural gas pipeline, Hendek (Turkey). *Environ Geol* 44(8):949–962
- Che VB, Kervyn M, Suh CE, Fontijn K, Ernst GGJ, del Marmol MA, Trefois P, Jacobs P (2012) Landslide susceptibility assessment in Limbe (SW Cameroon): a field calibrated seed cell and information value method. *Catena* 92:83–98
- Chen QX, Hu HT, Sun Y, Tan CX (1995) Assessment of regional crustal stability and its application to engineering geology in China. *Episodes* 18(1):69–72
- Chen YR, Chen JY, Hsieh SC, Ni PN (2009) The application of remote sensing technology to the interpretation of land use for rainfall-induced landslides based on genetic algorithms and artificial neural networks. *IEEE J-STARS* 2(2):87–95
- Chen T, Niu RQ, Li PX, Zhang LP, Du B (2011a) Regional soil erosion risk mapping using RUSLE, GIS, and remote sensing: a case study in Miyun Watershed, North China. *Environ Earth Sci* 63(3):533–541
- Chen T, Niu RQ, Wang Y, Li PX, Zhang LP, Du B (2011b) Assessment of spatial distribution of soil loss over the upper basin of Miyun reservoir in China based on RS and GIS techniques. *Environ Monit Assess* 179(1–4):605–617
- Chen T, Niu RQ, Du B, Wang Y (2015) Landslide spatial susceptibility mapping by using GIS and remote sensing techniques: a case study in Zigui County, the Three Georges reservoir, China. *Environ Earth Sci* 73(9):5571–5583
- Chung CJF, Fabbri AG (2003) Validation of spatial prediction models for landslide hazard mapping. *Nat Hazards* 30(3):451–472
- Dai FC, Lee CF, Xu ZW (2001) Assessment of landslide susceptibility on the natural terrain of Lantau Island, Hong Kong. *Environ Geol* 40(3):381–391
- Devkota KC, Regmi AD, Pourghasemi HR, Yoshida K, Pradhan B, Ryu IC, Dhital MR, Althuwaynee OF (2013) Landslide susceptibility mapping using certainty factor, index of entropy and logistic regression models in GIS and their comparison at Mugling-Narayanghat road section in Nepal Himalaya. *Nat Hazards* 65(1):135–165
- Duman TY, Can T, Gokceoglu C, Nefeslioglu HA, Sonmez H (2006) Application of logistic regression for landslide susceptibility zoning of Cekmece Area, Istanbul, Turkey. *Environ Geol* 51(2):241–256
- Fourniadis IG, Liu JG, Mason PJ (2007) Landslide hazard assessment in the Three Gorges area, China, using ASTER imagery: Wushan-Badong. *Geomorphology* 84(1):126–144
- Glade T (2003) Landslide occurrence as a response to land use change: a review of evidence from New Zealand. *Catena* 51(3):297–314

- Guzzetti F, Carrara A, Cardinali M, Reichenbach P (1999) Landslide hazard evaluation: a review of current techniques and their application in a multi-scale study, central Italy. *Geomorphology* 31(1):181–216
- He KQ, Li XR, Yan XQ, Guo D (2008) The landslides in the Three Gorges Reservoir Region, China and the effects of water storage and rain on their stability. *Environ Geol* 55(1):55–63
- Hosmer DW, Lemeshow S (2000) *Applied logistic regression*. Wiley, New York
- Hubei Province Geological Survey (1997) *Geological Map of Zigui and Badong County (1:50,000)* 1997 Hubei Province Geological Survey Press, Wuhan (in Chinese)
- Intrawichian N, Dasananda S (2011) Frequency ratio model based landslide susceptibility mapping in lower Mae Chaem watershed, Northern Thailand. *Environ Earth Sci* 64(8):2271–2285
- Kayastha P, Dhital MR, De Smedt F (2013) Evaluation and comparison of GIS based landslide susceptibility mapping procedures in Kulekhani watershed, Nepal. *J Geol Soc India* 81(2):219–231
- Lee S (2005) Application of logistic regression model and its validation for landslide susceptibility mapping using GIS and remote sensing data. *Int J Remote Sens* 26(7):1477–1491
- Lee S, Min K (2001) Statistical analysis of landslide susceptibility at Yongin, Korea. *Environ Geol* 40(9):1095–1113
- Lee S, Pradhan B (2007) Landslide hazard mapping at Selangor, Malaysia using frequency ratio and logistic regression models. *Landslides* 4(1):33–41
- Lee S, Choi J, Min K (2004) Probabilistic landslide hazard mapping using GIS and remote sensing data at Boun, Korea. *Int J Remote Sens* 25(11):2037–2052
- Li JJ, Xie SY, Kuang MS (2001) Geomorphic evolution of the Yangtze Gorges and the time of their formation. *Geomorphology* 41(2):125–135
- Liu JG, Mason PJ, Clerici N, Chen S, Davis A, Miao F, Deng H, Liang L (2004) Landslide hazard assessment in the Three Gorges area of the Yangtze River using ASTER imagery: Zigui-Badong. *Geomorphology* 61(1):171–187
- Liu CZ, Liu YH, Wen MS, Li TF, Lian JF, Qin SW (2009) *Geo-hazard initiation and assessment in the three gorges reservoir. Landslide Disaster Mitigation in Three Gorges Reservoir, China*. Springer, Berlin, pp 3–40
- Meentemeyer RK, Moody A (2000) Automated mapping of conformity between topographic and geological surfaces. *Comput Geosci* 26(7):815–829
- Nefeslioglu HA, Duman TY, Durmaz S (2008) Landslide susceptibility mapping for a part of tectonic Kelkit Valley (Eastern Black Sea region of Turkey). *Geomorphology* 94(3):401–418
- Nourani V, Pradhan B, Ghaffari H, Sharifi SS (2014) Landslide susceptibility mapping at Zonouz Plain, Iran using genetic programming and comparison with frequency ratio, logistic regression, and artificial neural network models. *Nat Hazards* 71(1):523–547
- Oh HJ, Kim YS, Choi JK, Lee S (2011) GIS mapping of regional probabilistic groundwater potential in the area of Pohang City, Korea. *J Hydrol* 399(3):158–172
- Ozdemir A, Altural T (2013) A comparative study of frequency ratio, weights of evidence and logistic regression methods for landslide susceptibility mapping: Sultan Mountains, SW Turkey. *J Asian Earth Sci* 64:180–197
- Papadopoulou-Vrynioti K, Bathrellos GD, Skilodimou HD, Kaviris G, Makropoulos K (2013) Karst collapse susceptibility mapping using seismic hazard in a rapid urban growing area. *Eng Geol* 158:77–88
- Peng L, Niu RQ, Huang B, Wu XL, Zhao YN, Ye RQ (2014) Landslide susceptibility mapping based on rough set theory and support vector machines: a case of the Three Gorges area, China. *Geomorphology* 204:287–301
- Pourghasemi HR, Pradhan B, Gokceoglu C, Mohammadi M, Moradi HR (2013) Application of weights-of-evidence and certainty factor models and their comparison in landslide susceptibility mapping at Haraz watershed, Iran. *Arab J Geosci* 6(7):2351–2365
- Pourghasemi HR, Moradi HR, Aghda SMF, Gokceoglu C, Pradhan B (2014) GIS-based landslide susceptibility mapping with probabilistic likelihood ratio and spatial multi-criteria evaluation models (North of Tehran, Iran). *Arab J Geosci* 7(5):1857–1878
- Pradhan B (2010) Landslide susceptibility mapping of a catchment area using frequency ratio, fuzzy logic and multivariate logistic regression approaches. *J Indian Soc Remote Sens* 38(2):301–320
- Pradhan B (2013) A comparative study on the predictive ability of the decision tree, support vector machine and neuro-fuzzy models in landslide susceptibility mapping using GIS. *Comput Geosci* 51:350–365
- Pradhan B, Lee S (2010) Delineation of landslide hazard areas on Penang Island, Malaysia, by using frequency ratio, logistic regression, and artificial neural network models. *Environ Earth Sci* 60(5):1037–1054
- Pradhan B, Mansor S, Pirasteh S, Buchroithner F (2011) Landslide hazard and risk analyses at a landslide prone catchment area using statistical based geospatial model. *Int J Remote Sens* 32(14):4075–4087
- Ramakrishnan D, Ghose MK, Chandran RV, Jeyaram A (2005) Probabilistic techniques, GIS and remote sensing in landslide hazard mitigation: a case study from Sikkim Himalayas, India. *Geocarto Int* 20(4):53–58
- Regmi AD, Devkota KC, Yoshida K, Pradhan B, Pourghasemi HR, Kumamoto T, Akgun A (2014) Application of frequency ratio, statistical index, and weights-of-evidence models and their comparison in landslide susceptibility mapping in Central Nepal Himalaya. *Arab J Geosci* 7(2):725–742
- Rozos D, Bathrellos GD, Skilodimou HD (2011) Comparison of the implementation of Rock Engineering System (RES) and Analytical Hierarchy Process (AHP) methods, based on landslide susceptibility maps, compiled in GIS environment. A case study from the Eastern Achaia County of Peloponnesus, Greece. *Environ Earth Sci* 63(1):49–63
- Rozos D, Skilodimou HD, Loupasakis C, Bathrellos GD (2013) Application of the revised universal soil loss equation model on landslide prevention. An example from N. Euboea (Evia) Island, Greece. *Environ Earth Sci* 70(7):3255–3266
- Sarkar S, Roy AK, Martha TR (2013) Landslide susceptibility assessment using Information Value Method in parts of the Darjeeling Himalayas. *J Geol Soc India* 82(4):351–362
- Shahabi H, Khezri S, Ahmad BB, Hashim M (2014) Landslide susceptibility mapping at central Zab basin, Iran: a comparison between analytical hierarchy process, frequency ratio and logistic regression models. *Catena* 115:55–70
- Süzen ML (2002) *Data driven landslide hazard assessment using geographical information systems and remote sensing*. PhD Thesis, Middle East Technical University, Turkey
- Süzen ML, Doyuran V (2004) A Comparison of the GIS based landslide susceptibility assessment methods: multivariate versus bivariate. *Environ Geol* 45(5):665–679
- Swets JA (1988) Measuring the accuracy of diagnostic systems. *Science* 240(4857):1285–1293
- Talebi A, Uijlenhoet R, Troch PA (2007) Soil moisture storage and hillslope stability. *Nat Hazards Earth Syst Sci* 7(5):523–534
- Vijith H, Rejith PG, Madhu G (2009) Using InfoVal method and GIS techniques for the spatial modelling of landslide susceptibility in the upper catchment of river Meenachil in Kerala. *J Indian Soc Remote Sens* 37(2):241–250

- Wen BP, Wang SJ, Wang EZ, Zhang JM (2004) Characteristics of rapid giant landslides in China. *Landslides* 1(4):247–261
- Wilson JP, Gallant JC (2000) *Terrain analysis principles and applications*. Wiley, New York
- Wu SR, Shi L, Wang RJ, Tan CX, Hu DG, Mei YT, Xu RC (2001) Zonation of the landslide hazards in the forereservoir region of the Three Gorges Project on the Yangtze River. *Eng Geol* 59(1):51–58
- Wu SR, Jin YM, Zhang YS, Shi JS, Dong C, Lei WZ, Shi L, Tan CX, Hu DG (2004) Investigations and assessment of the landslide hazards of Fengdu County in the reservoir region of the Three Gorges project on the Yangtze River. *Environ Geol* 45(4):560–566
- Yan TZ (1988) Recent advances of quantitative prognoses of landslide in China. In: *Proceedings of the fifth international symposium on landslides*, Lausanne, Switzerland, vol 2, pp 1263–1268
- Yesilnacar E, Topal T (2005) Landslide susceptibility mapping: a comparison of logistic regression and neural networks methods in a medium scale study, Hendek region (Turkey). *Eng Geol* 79(3):251–266
- Yin KL, Yan TZ (1988) Statistical prediction models for slope instability of metamorphosed rocks. In: *Proceedings of the fifth international symposium on landslides*, Lausanne, Switzerland, vol 2, pp 1269–1272
- Youssef AM, Maerz NH (2013) Overview of some geological hazards in the Saudi Arabia. *Environ Earth Sci* 70(7):3115–3130